Magnetoelectricity in the ferrimagnetic Cu_2OSeO_3: symmetry analysis and Raman scattering study

V.P. Gnezdilov[1], K.V. Lamonova[2], Yu.G. Pashkevich[2], P. Lemmens[3],

H. Berger[4], F. Bussy[5], and S.L. Gnatchenko[1]

[1]*B. Verkin Institute for Low Temperature Physics and Engineering of the National Academy of Sciences of Ukraine*
47 Lenin Ave., Kharkov 61103, Ukraine
E-mail: gnezdilov@ilt.kharkov.ua

[2]*A.A. Galkin Donetsk Phystech of the National Academy of Sciences of Ukraine, Donetsk 83114, Ukraine*
[3]*Institute for Condensed Matter Physics, TU Braunschweig, D-38106 Braunschweig, Germany*
[4]*Institute of Condensed Matter Physics, Ecole Polytechnique Fédérale de Lausanne,*
CH-1015, Lausanne, Switzerland
[5]*Institute of Mineralogy and Geochemistry, ANTHROPOLE, University of Lausanne,*
CH-1015 Lausanne, Switzerland

We report Raman scattering studies and magneto/structural symmetry analysis of the many sublattices ferrimagnet Cu_2OSeO_3 with a cubic symmetry and a linear magnetoelectric effect. There is no spectroscopic evidence for structural lattice distortions below $T_C = 60$ K, which are expected due to magnetoelectric coupling. Using symmetry arguments we explain this observation by considering a special type of ferrimagnetic ground state which does not generate a spontaneous electric polarization. Interestingly, Raman scattering shows a strong increase of electric polarization of media through a dynamic magnetoelectric effect as a remarkable enhancement of the scattering intensity below T_C. New lines of purely magnetic origin have been detected in the magnetically ordered state. A part of them are attributed as scattering on exchange magnons. Using this observation and further symmetry considerations we argue for strong Dzyaloshinskii–Moriya interaction existing in the Cu_2OSeO_3.

1. Introduction

Cu_2OSeO_3 represents one of the less common copper oxides in which ferrimagnetic order is realized [1,2]. Besides, in the paramagnetic phase it has high cubic symmetry but without showing inversion symmetry (space group $P2_13$) [2–4]. This space group does not allow electric polarization in the paramagnetic phase but it permits a linear magnetoelectric (ME) effect in the magnetically ordered state. In a recent paper of J.-W. Bos *et al*. [2] significant magnetocapacitance in Cu_2OSeO_3 has been observed. The temperature dependence of dielectric constants demonstrates an unexpected anomaly with an enhancement just below the Curie temperature ($T_C = 60$ K)

and some suppression below $T^* = 20$ K that is in complete contrast to the lattice thermal expansion. Moreover, high-resolution x-ray and neutron powder diffraction measurements have not found a measurable spontaneous structural distortions in the magnetically ordered state. This means that the sample remains metrically cubic down to low temperatures (10 K) [2]. This fact excludes the possibility of ME coupling in Cu_2OSeO_3 via a spontaneous lattice distortion for temperatures below T_C.

A purely «electronic mechanism» of magnetoelectricity (here we use the terminology of a recent review paper [5]) does not occur so often in nature while there are many multiferroic materials where magnetoelectric coupling is associated with lattice distortions [6–10]. So, further

investigations and a theoretical analysis of the Cu_2OSeO_3 system are needed for the purpose of understanding its unusual magnetoelectric coupling mechanism. To elucidate possible manifestations of so far unobserved lattice distortions we apply the Raman scattering (RS) technique. Raman spectroscopy is very sensitive tool for the detection local structural changes by investigation of elementary excitations of the lattice and spin systems of solids ([11] and references therein). Strong coupling between the lattice and spin degrees of freedom offer the possibility of probing the order and dynamics of both systems and as well their interaction.

Here, we present the results of our RS investigation into the intriguing system of Cu_2OSeO_3. The main observation is the appearance of new lines in the Raman spectra of Cu_2OSeO_3 with cooling through the magnetic ordering temperature T_C and T^*, the temperature below which the dielectric constant shows a value smaller than the extrapolated lattice contribution [2]. The origin of new lines is discussed. Our spectra do not demonstrate effects that can be interpreted as due to spontaneous lattice distortions in Cu_2OSeO_3. The earlier observed additional magnetoelectric polarizability of the compound manifests itself as a general enhancement of the phonon integrated scattering intensities below T_C.

In a Landau theory approach we performed a complete symmetry analysis of the magnetic degrees of freedom and the magnetoelectric coupling in Cu_2OSeO_3. We show that the structural features of the magnetic bonds allow strong Dzyaloshinskii–Moriya (DM) interactions and the appearance of antiferromagnetic components in the ferrimagnetic state. Assuming a sufficient canting of the ferrimagnetic structure, one can explain the low magnitude of the saturation magnetic moment (0.5 μ_B/Cu) observed in high magnetic field [2]. The magnetoelectric coupling is realized trough both Heisenberg-exchange and relativistic type mechanisms. The former term includes a scalar product of the ferromagnetic and DM induced antiferromagnetic vectors. We show that magnetoelectric energy can be rewritten in terms of the sublattices ferromagnetic moments and the form of magnetoelectric tensors does not allow the appearance of spontaneous electric polarizations for some specific directions of the net ferrimagnetic moments.

2. Experimental details

Single crystals of Cu_2OSeO_3 have been grown by standard chemical vapour phase method. Mixtures of high purity CuO (Alfa-Aesar, 99.995%) and SeO_2 (Alfa-Aesar, 99.999%) powder in molar ratio 2 : 1 were sealed in the quartz tubes with electronic grade HCl as the transport gas for the crystal growth. The ampoules were then placed horizontally into a tubular two-zone furnaces and heated very slowly by 50 °C/h to 600 °C. The optimum temperatures at the source and deposition zones for the growth of the single crystals have been 610 and 500 °C, respectively.

After six weeks, many dark green, almost black Cu_2OSeO_3 crystals with a maximum size of $8 \times 6 \times 3$ mm were obtained. X-ray powder diffraction (XRD) analysis was conducted on a Rigaku x-ray diffractometer with CuK_α radiation ($\lambda = 1.5418$ Å) and electron microprobe was used for chemical analysis of all solid samples.

The RS experiments were performed in a quasi-back-scattering geometry on the as-grown, shiny (111) surfaces of Cu_2OSeO_3 single crystals. We used the excitation wavelengths $\lambda = 514.5$ nm of an Ar/Kr ion laser and $\lambda = 532.1$ nm of a solid-state laser with a power level $P = 5$ mW. The scattered light was collected in quasi-backscattering configuration and dispersed by a triple monochromator DILOR XY on a liquid-nitrogen-cooled CCD detector. In our experiments we used parallel (*XX*) and crossed (*XY*) light polarizations. Temperature dependencies were measured in a variable temperature closed cycle cryostat (Oxford/Cryomech Optistat, RT-2.8 K).

3. Results and discussion

3.1. Structural and magnetic features of Cu_2OSeO_3

Cu^{2+} ferrimagnetic order in Cu_2OSeO_3 sets in at about $T_C = 60$ K [1,2]. Note that ferrimagnetic order implies the absence of the magnetic primitive cell multiplication. The space group of the paramagnetic phase is cubic $P2_13$ with eight formula units per cell [2–4]. The sixteen Cu^{2+} ions are distributed among two 4a (CuI type — C_3 site symmetry) and 12b (CuII type — general site) positions. Here and in the next we accept ion-site's enumeration which has been proposed in Ref. 2. The Cu^{2+} ions form a network of distorted tetrahedra shown in Fig. 1 (right) so that the nearest neighbor exchange interaction between CuI–CuI sites is absent. The topology of magnetic bonds is dictated by almost undistorted trigonal bipyramids $CuIO_5$ and strongly distorted square pyramids $CuIIO_5$ and part of the representatives are shown in Fig. 2. The remarkable and further general features of the Cu_2OSeO_3 structure are:

1) closeness almost of all Cu–O–Cu bond angles to 90°, which results to the appearance of ferromagnetic exchange interactions [12,13];

2) strongly asymmetric pairs of Cu-O-Cu bonds or even lone Cu–O–Cu bonds connecting nearest neighbor copper ions, which leads to the presence of strong Dzyaloshinskii–Moriya interactions.

Due to the difference in distances, there are two distinctive magnetic bonds for both CuI–CuII and CuII–CuII magnetic interactions. One can consider the features of these bonds by the example of ions group shown in Fig. 2. In the edge shared $CuIO_5 - CuIIO_5$ polyhedra (the CuI–CuII distances are 3.049 Å) there are two magnetic bonds with bond angles $\angle Cu1–O1–CuIx = 104.72°$ and $\angle Cu1–O3–CuIx = 96.17°$. These angles are the same for replacement x indexes into y and z as well under change of CuI numbers. For corner shared $CuIO_5 - CuIIO_5$ polyhedra (the CuI–CuII
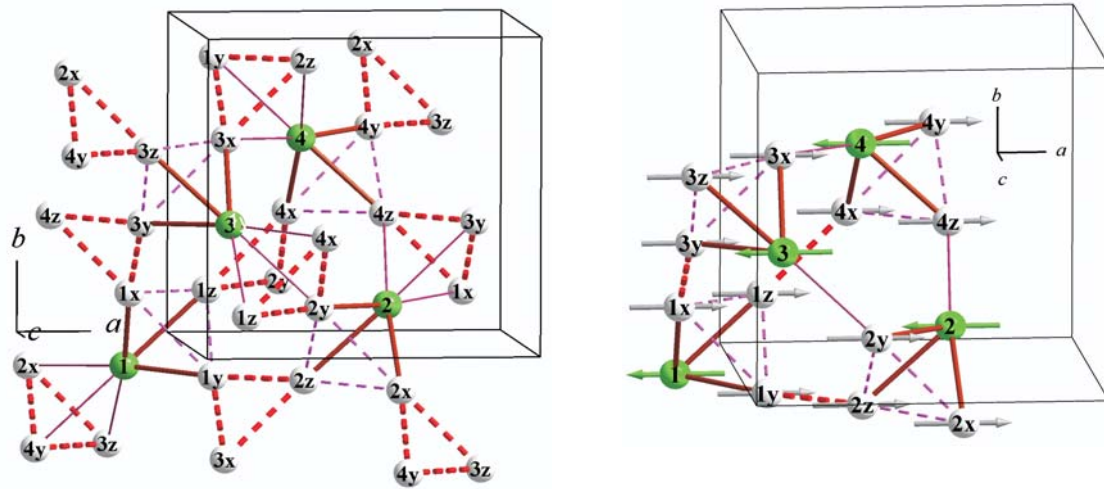
Fig. 1. (Left) Network of Cu ions in Cu_2OSeO_3. Dark and light balls are CuI (from 4a site) and CuII (from 12b site) types of magnetic ions, respectively. Solid thin and thick lines connect CuI–CuII neighbors on short (3.049 Å) and long (3.304 Å) distances, respectively. Dotted thin and thick lines connect CuII–CuII neighbors on short (3.054 Å) and long (3.226 Å) distances, respectively. Proposed enumeration of the magnetic ions is shown. The numbers of CuII ions are chosen on the basis of the closeness to the nearest Cu1 ions with additional Cartesian indices. (Right) Cu_2OSeO_3 magnetic structure of the $P2_1$ type with ferrimagnetic moment directed along (100) direction [2].

distances are 3.304 Å) there is the only magnetic bond through the O2 type oxygen with bond angle $\angle Cu1–O2–Cu2x = 116.5°$ with replacement Cu2x into Cu3z and Cu4y. In the edge shared $CuIIO_5$ pyramids (the CuII–CuII distances are 3.054 Å) there are two magnetic bonds with bond angles $\angle Cu2x–O2–Cu4y = 101.62°$ and $\angle Cu2x–O4–Cu4y = 91.68°$. For the corner shared $CuIIO_5$ pyramids (the CuII–CuII distances are 3.226 Å) there is the only magnetic bond through the O1 type oxygen with bond angles $\angle Cu1x–O1–Cu1x = 113.77°$.
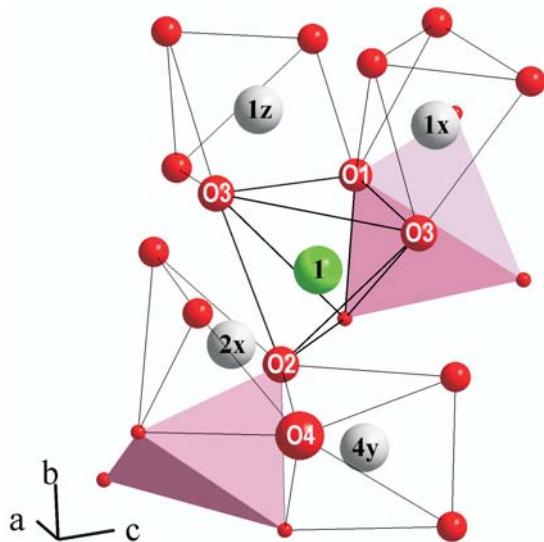

Fig. 2. Illustration of the magnetic bond patterns for CuI–CuII and CuII–CuII magnetic interactions. The enumeration of oxygen ions is the same as in the Ref. 2, i.e., O1 and O2 belong to the 4a positions while O3 and O4 belong to the 12b positions.

Thus, in spite of sixteen sublattices, exchange magnetic interactions in Cu_2OSeO_3 (in nearest-neighbor approximation) can be described just by four exchange integrals. They are: two exchanges between CuI–CuII sites and two exchanges between CuII–CuII sites (see Fig. 1 (left)). A close inspection of distances and angles leads to the conclusion that we deal with the following type of exchange integrals:

I) J_F^{12} CuI–(O1+O3)–CuII {3.049 Å};

II) J_{AF}^{12} CuI–O2–CuII {3.304 Å};

III) J_F^{22} CuII–(O2+O4)–CuII {3.054 Å};

IV) J_{AF}^{22} CuII–O1–CuII {3.226 Å}.

Here, ferromagnetic exchange $J_F < 0$ and antiferromagnetic exchange $J_{AF} > 0$, in the parenthesizes the oxygen ions are shown trough which the magnetic bonds are realized, the Cu–Cu distances are given in the braces. Note that there is no consensus about the critical angles of Cu–O–Cu magnetic bonds at which magnetic exchange changes sign ([12,13], and discussion in [14]). Therefore, our attribution of CuI–CuII (3.049 Å) exchange to the ferromagnetic one has to be confirmed by further calculations.

To analyze the symmetry of the magnetic degrees of freedom we introduce linear combinations of the CuI sublattices spin $\mathbf{s}_\alpha$ and the CuII sublattices spin $\mathbf{s}_\alpha^{(i)}$ where $\alpha = 1-4$ and index $i = x, y, z$ enumerates three groups of twelve CuII ions (see enumeration in Fig. 1):

$$\mathbf{F}_I = 1/4(\mathbf{s}_1 + \mathbf{s}_2 + \mathbf{s}_3 + \mathbf{s}_4); \quad \mathbf{F}^{(i)} = 1/4(\mathbf{s}_1^{(i)} + \mathbf{s}_2^{(i)} + \mathbf{s}_3^{(i)} + \mathbf{s}_4^{(i)});$$

$$\mathbf{L}_1 = 1/4(\mathbf{s}_1 + \mathbf{s}_2 - \mathbf{s}_3 - \mathbf{s}_4); \quad \mathbf{L}_1^{(i)} = 1/4(\mathbf{s}_1^{(i)} + \mathbf{s}_2^{(i)} - \mathbf{s}_3^{(i)} - \mathbf{s}_4^{(i)});$$

$$\mathbf{L}_2 = 1/4(\mathbf{s}_1 - \mathbf{s}_2 + \mathbf{s}_3 - \mathbf{s}_4); \quad \mathbf{L}_2^{(i)} = 1/4(\mathbf{s}_1^{(i)} - \mathbf{s}_2^{(i)} + \mathbf{s}_3^{(i)} - \mathbf{s}_4^{(i)});$$

$$\mathbf{L}_3 = 1/4(\mathbf{s}_1 - \mathbf{s}_2 - \mathbf{s}_3 + \mathbf{s}_4); \quad \mathbf{L}_3^{(i)} = 1/4(\mathbf{s}_1^{(i)} - \mathbf{s}_2^{(i)} - \mathbf{s}_3^{(i)} + \mathbf{s}_4^{(i)});$$

$$\mathbf{F}_{II} = \mathbf{F}^{(x)} + \mathbf{F}^{(y)} + \mathbf{F}^{(z)}. \tag{1}$$

Here $\mathbf{F}_I$ and $\mathbf{F}_{II}$ are «ferromagnetism vectors» of the CuI and CuII sublattices. In a case of a second-order magnetic phase transition, the possible magnetic structures can be classified by the irreducible representations (IR) of the symmetry group of the crystal in the paramagnetic phase. The basis functions of IR are formed from Cartesian components of vectors (1) (see Table A in the Appendix). Exchange interactions have higher exchange symmetry because of the scalar product of magnetic moments depends just on the mutual angles between them. The symmetry of exchange multiplets are listed in Table 1.

Using the data of Table 1 one can obtain the exchange part of the magnetic Hamiltonian in nearest–neighbor approximation:

$$
\begin{aligned}
H = {} & 4\left(J_F^{12} + J_{AF}^{12}\right)\left[\mathbf{F}_I \cdot \mathbf{F}_{II} + \mathbf{L}_3 \cdot \mathbf{L}_3^{(y)} + \mathbf{L}_2 \cdot \mathbf{L}_2^{(z)} + \mathbf{L}_1 \cdot \mathbf{L}_1^{(x)}\right] + \\
& + 4\left(J_F^{12} - J_{AF}^{12}\right)\left[\mathbf{L}_3 \cdot \left(\mathbf{L}_3^{(x)} + \mathbf{L}_3^{(z)}\right) + \mathbf{L}_2 \cdot \left(\mathbf{L}_2^{(y)} + \mathbf{L}_2^{(x)}\right) + \mathbf{L}_1 \cdot \left(\mathbf{L}_1^{(z)} + \mathbf{L}_1^{(y)}\right)\right] + \\
& + 4\left(J_F^{22} + J_{AF}^{22}\right)\left[\mathbf{F}^{(x)} \cdot \mathbf{F}^{(z)} + \mathbf{F}^{(y)} \cdot \mathbf{F}^{(z)} + \mathbf{F}^{(x)} \cdot \mathbf{F}^{(y)} + \mathbf{L}_3^{(x)} \cdot \mathbf{L}_3^{(z)} + \mathbf{L}_2^{(y)} \cdot \mathbf{L}_2^{(x)} + \mathbf{L}_1^{(z)} \cdot \mathbf{L}_1^{(y)}\right] + \\
& + 4\left(-J_F^{22} + J_{AF}^{22}\right)\left[\mathbf{L}_3^{(y)} \cdot \left(\mathbf{L}_3^{(x)} + \mathbf{L}_3^{(z)}\right) + \mathbf{L}_2^{(z)} \cdot \left(\mathbf{L}_2^{(y)} + \mathbf{L}_2^{(x)}\right) + \mathbf{L}_1^{(x)} \cdot \left(\mathbf{L}_1^{(z)} + \mathbf{L}_1^{(y)}\right)\right].
\end{aligned} \tag{2}
$$

As follows from (2) ferrimagnetic order in Cu_2OSeO_3 exists under the condition:

$$J_F^{22} + J_{AF}^{22} - J_F^{12} - J_{AF}^{12} < 0. \tag{3}$$

The topology of the magnetic bonds also dictates some features of the main exchange magnetic contribution to the dielectric constant. In the case of ferrimagnetic ground state it should contain two competing parts arising from invariants $\mathbf{F}_I \cdot \mathbf{F}_{II}$ and $\mathbf{F}_{II}^2$. Probably, this competition can explain the unusual temperature dependence of the dielectric permeability Cu_2OSeO_3 below T_C (see Fig. 6,*a* in Ref. 2).

In Cu_2OSeO_3 the arrangement of every kind of Cu–Cu magnetic bonds allows Dzyaloshinskii–Moriya interacttions, *D*. Usual estimations of the DM magnitude is $D \propto (\Delta g / g)J$ where Δg is deviation of the *g*-factor from free electron value $g_0 = 2$ and *J* is the exchange interaction. Our preliminary calculations show that most strong deviations of *g*-factor occur in the strongly distorted square pyramids $CuIIO_5$. In the ferrimagnetic state with the ferromagnetism vectors $\mathbf{F}_I$ and $\mathbf{F}_{II}$ aligned along (111) direction (see Fig. 5,*b* in [2]) almost all components of all type of $\mathbf{L}$ vectors are induced by DM interactions. Respective invariants in the Hamiltonian can be easily obtained using Table A from the Appendix. Only 3_{111} and 3_{111}^{-1} symmetry operations survive after magnetic ordering (unitary subgroup of the magnetic group is *R*3 [2]) and both CuI (4*a*) and CuII (12*b*) positions split into two and four independent sets, respectively. For instance, there are two sets of CuI positions: a first one with only one Cu1 ion and a second one with three Cu2, Cu3 and Cu4 ions. One

Table 1. The transformation properties of the Cu_2OSeO_3 exchange multiplets (1) and Cartesian components of electric polarization **P** under symmetry operations of the paramagnetic phase $P2_13$ space group. The first column displays irreducible representations. $\varepsilon = \exp(i2\pi/3)$

IR	**P**	Exchange multiplets		Symmetry of bilinear terms which induce exchange magnetoelectric invariants caused by CuI–CuII interactions			
		CuI	CuII				
A	–	$\mathbf{F}_I$	$\mathbf{F}_{II} = \mathbf{F}^{(x)} + \mathbf{F}^{(y)} + \mathbf{F}^{(z)}$	–			
E_1	–	–	$\mathbf{F}^{(z)} + \varepsilon\mathbf{F}^{(y)} + \varepsilon^2\mathbf{F}^{(x)}$	–			
E_2	–	–	$\mathbf{F}^{(z)} + \varepsilon^2\mathbf{F}^{(y)} + \varepsilon\mathbf{F}^{(x)}$	–			
T	$\begin{cases} P_x \\ P_y \\ P_z \end{cases}$	$\begin{cases} \mathbf{L}_3 \\ \mathbf{L}_2 \\ \mathbf{L}_1 \end{cases}$	$\begin{cases} \mathbf{L}_3^{(z)} \\ \mathbf{L}_2^{(x)} \\ \mathbf{L}_1^{(y)} \end{cases}$; $\begin{cases} \mathbf{L}_3^{(y)} \\ \mathbf{L}_2^{(z)} \\ \mathbf{L}_1^{(x)} \end{cases}$; $\begin{cases} \mathbf{L}_3^{(x)} \\ \mathbf{L}_2^{(y)} \\ \mathbf{L}_1^{(z)} \end{cases}$	$\begin{cases} \mathbf{F}_I\mathbf{L}_3^{(z)} \\ \mathbf{F}_I\mathbf{L}_2^{(x)} \\ \mathbf{F}_I\mathbf{L}_1^{(y)} \end{cases}$	$\begin{cases} \mathbf{F}_I\mathbf{L}_3^{(y)} \\ \mathbf{F}_I\mathbf{L}_2^{(z)} \\ \mathbf{F}_I\mathbf{L}_1^{(x)} \end{cases}$;	$\begin{cases} \mathbf{F}_I\mathbf{L}_3^{(x)} \\ \mathbf{F}_I\mathbf{L}_2^{(y)} \\ \mathbf{F}_I\mathbf{L}_1^{(z)} \end{cases}$;	$\begin{cases} \mathbf{F}_{II}\mathbf{L}_3 \\ \mathbf{F}_{II}\mathbf{L}_2 \\ \mathbf{F}_{II}\mathbf{L}_1 \end{cases}$

can show that at the given type of the three-component magnetic order parameter the Cu^{2+} ions from different sets have different saturation moments caused by DM interaction. Thus, due to this and due to spin-canting the DM interactions in Cu_2OSeO_3 should suppress a net ferrimagnetic moment as it really observed in experiment of J.-W. Bos *et al.* [2].

3.2. Magnetoelectricity in Cu_2OSeO_3

Since the classical review of G.A. Smolenskii and I.E. Chupis [15] the exchange and relativistic origin of the linear ME phenomenon are well appreciated. Exchange interactions have higher symmetry than exact magnetic symmetry; therefore the exchange contribution to the magnetoelectric constant can be prohibited while the relativistic one can survive. Symmetry conditions for the existence of magnetoelectric effects of exchange nature in antiferromagnets have been considered in Ref. 16. Formally in the ferrimagnetic Cu_2OSeO_3 there is the presence of both contributions to the linear ME effect. In the Landau approach the relativistic part of ME energy has the standard form in accordance with cubic $P2_13$ symmetry:

$$P_x[\alpha F_{Iy}F_{IIz} + \beta F_{Iz}F_{IIy} + \gamma F_{IIy}F_{IIz}],$$
$$P_y[\alpha F_{Iz}F_{IIx} + \beta F_{Ix}F_{IIz} + \gamma F_{IIz}F_{IIx}], \quad (4)$$
$$P_z[\alpha F_{Ix}F_{IIy} + \beta F_{Iy}F_{IIz} + \gamma F_{IIx}F_{IIy}].$$

Some representatives of exchange part contributions arising from interactions of CuI–CuII pairs of ions can be written with help of the right column of Table 1:

$$P_x[(aL_3^{(z)} + bL_3^{(y)} + cL_3^{(x)})F_I + dF_{II}L_3)],$$
$$P_y[(aL_2^{(x)} + bL_2^{(z)} + cL_2^{(y)})F_I + dF_{II}L_2], \quad (5)$$
$$P_z[(aL_1^{(y)} + bL_1^{(x)} + cL_1^{(z)})F_I + dF_{II}L_1].$$

Also exchange invariants originating from CuII–CuII pairs should be added to the ME energy (5). However, all nonzero components of antiferromagnetic vectors L are induced by ferromagnetic moments trough DM interacttions. In other way, they have the form $L_i \propto (D_l / J) | e_{ilj} | F_j$ (here i, j, l are Cartesian indexes, e_{ilj} is the fully asymmetric tensor, D

the vector of DM interaction, the non-Cartesian indexes are omitted for clarity). One can show that after substitution of L components by F_I and F_{II} components in (5) this exchange part of contribution to ME effect gains the same form as relativistic one (4), i.e., exchange contribution to the ME effect leads only to the renormalization of the α, β, γ constants in the relativistic part (4).

This conclusion about the form of ME effect does not depend on the origin of the net magnetic moment in space. Note, that in Ref. 2 also possible magnetic structure of Cu_2OSeO_3 are discussed with an orientation of the net magnetic moment along (100) direction (see Fig. 1 (right)). As follows from expression (4) in this case spontaneous electric polarization will be absent. While in the *powder* sample some magnetocapacitance should be seen under action of a magnetic field and an alignment of the net magnetic moment along the field. Moreover, the magnetocapacitance should start to increase at some critical field when the net ferrimagnetic moment starts to rotate from its easy axis to the direction of a magnetic field. Such a scenario is really seen in the experiment (see Fig. 7,*a* in Ref. 2). However, the observed behavior of magnetocapacitance evidences also some complex field induced spin reorientation in Cu_2OSeO_3. To make more definite conclusions about features of magnetoelectricity in Cu_2OSeO_3 experiments on single crystal are needed.

3.3. Symmetry of phonons and magnons in Cu_2OSeO_3

For an analysis of the coupling between the lattice and spin degrees of freedom a complete knowledge of the vibration properties of the materials under investigation is necessary. For the cubic structure of Cu_2OSeO_3 (space group $P2_13$, N198, $Z = 8$ with five ions in 4a positions and three ions in 12b position [2–4]), the factor group analysis gives following types of phonons:

$$\Gamma = 14A + 14E_1 + 14E_2 \quad \text{(Raman-active)},$$
$$+42T \quad \text{(IR- and Raman-active)}.$$

The Raman tensors take the form:

$$\begin{pmatrix} a & 0 & 0 \\ 0 & a & 0 \\ 0 & 0 & a \end{pmatrix} \begin{pmatrix} b+\sqrt{3}c & 0 & 0 \\ 0 & b-\sqrt{3}c & 0 \\ 0 & 0 & -2b \end{pmatrix} \begin{pmatrix} c-\sqrt{3}b & 0 & 0 \\ 0 & c+\sqrt{3}b & 0 \\ 0 & 0 & -2c \end{pmatrix} \begin{pmatrix} 0 & 0 & 0 \\ 0 & 0 & d \\ 0 & d & 0 \end{pmatrix} \begin{pmatrix} 0 & 0 & d \\ 0 & 0 & 0 \\ d & 0 & 0 \end{pmatrix} \begin{pmatrix} 0 & d & 0 \\ d & 0 & 0 \\ 0 & 0 & 0 \end{pmatrix}.$$

$$A \qquad E_1 \qquad E_2 \qquad T(x) \quad T(y) \quad T(z)$$

The number of magnons equals to σ, the number of magnetic sublattices. This is caused by conservation of modulus of magnetic moments and the same energy for sublattices with right and left spin precession. The symmetry

of magnon's modes can be obtained from an analysis of Γ_{SW}, the spin wave representation with $2\sigma \times 2\sigma$ dimension [17]. Using the symmetry of unitary subgroup $R3$ for ferrimagnetic order with net magnetization along (111) we
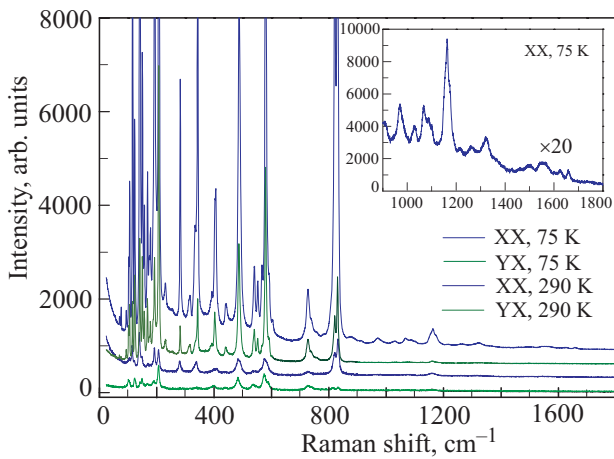
Fig. 3. Raman spectra of single crystal Cu$_2$OSeO$_3$ at temperatures above T_C = 60 K in two scattering geometries. Inset shows a zoomed-in *XX*-spectrum at *T* = 75 K in the frequency region 900–1800 cm^{-1}.

Fig. 4. Temperature dependent Raman spectra of Cu$_2$OSeO$_3$.

obtain $5\tilde{A} + 11\tilde{E}$ magnon modes, here $\tilde{A}$ and $\tilde{E}$ are IR of the $R3$ group with Z' axis directed along (111). For the case of ferrimagnetic moment directed along (100) we have the symmetry of magnon modes $8A' + 8B'$ where A' and B' are the IR of the unitary subgroup $P2_1$ of the magnetic group $P2_12_1'2_1'$ ascribed in Ref. 2. One of the $\tilde{E}$ (or B') modes is an acoustic mode with a small energy gap defined by the anisotropy, while other ones are exchange modes (an analogue of optic phonons) with energies determined by exchange interactions. The exchange integrals in Cu$_2$OSeO$_3$ are unknown but from T_C = 60 K one can estimate the energy region of exchange modes up to a few hundreds of wave numbers.
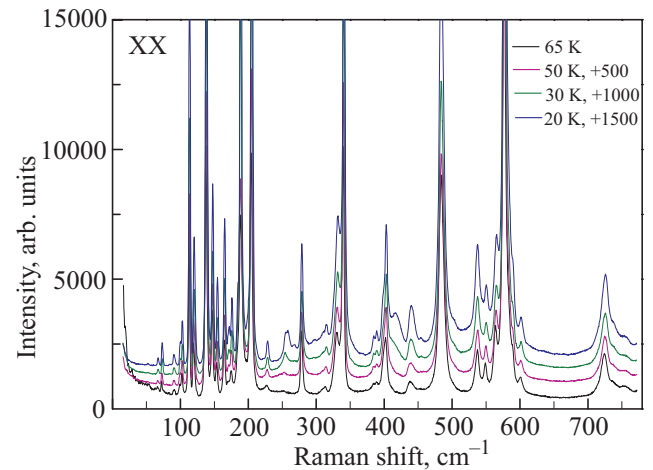
3.4. Raman spectra of Cu$_2$OSeO$_3$

Raman spectra of Cu$_2$OSeO$_3$ at temperatures 290 and 75 K are presented in Fig. 3. Narrow and well-distinguishable phonon peaks (that testify the high quality of the investigated samples) with different intensities are observed in the spectra. Of the total 84 Γ-point Raman-active phonon modes, 53 phonon lines can be surely identified in the frequency regime 0–850 cm^{-1}. Besides, as minimum 21 weak phonon lines are observed in the higher frequency regime up to 2000 cm^{-1}.

The temperature dependence of the Raman spectra of Cu$_2$OSeO$_3$ in Fig. 4 and the results of a temperature analysis in Fig. 5 show several distinctive features. First, all phonon lines show anomalies at T_C in their eigenfrequencies, integrated intensities, and linewidths that indicate strong
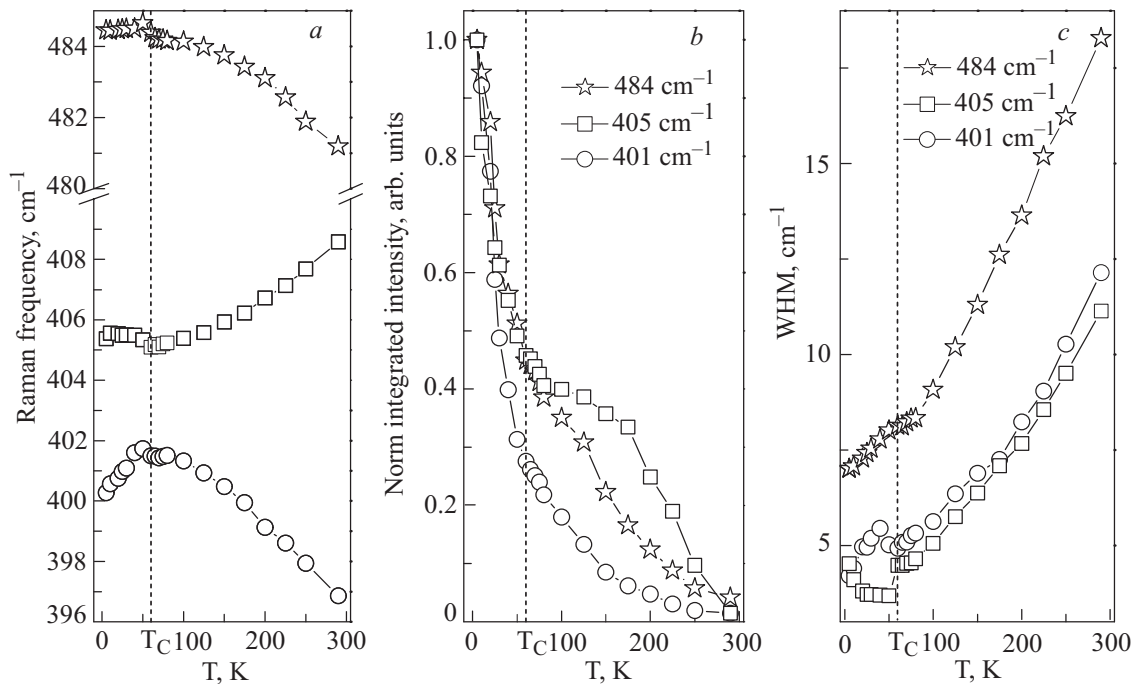

Fig. 5. Temperature dependencies of the eigenfrequencies (*a*), normalized integrated intensities (*b*), and widths (*c*) of the selected phonon lines in Cu$_2$OSeO$_3$.

spin-lattice coupling in Cu_2OSeO_3. The most remarkable is the pronounced enhancement of phonon integrated intensities below T_C. Such behavior can be unambiguously attributed to an increase of the dynamic electric polarizability of media due to some contribution of the ME effect.

Second and most intriguing, 3 new lines at frequencies of ~261, 270, and 420 cm^{-1} abruptly appear upon cooling below the ferrimagnetic ordering temperature T_C, see Fig. 6. These new lines have a strong and unusual temperature dependence in their parameters: energy, intensity, and width, compared with the original phonon lines. Some possible explanations for these new lines, appearing in both scattering geometries, such as phonon lines induced by magnetic ordering and symmetry lowering can be ruled out by following arguments. The lattice primitive cell does not change under ferrimagnetic order, therefore no phonon modes from the Brillouin zone boundary should be induced. All type of phonon modes from Γ-point are already allowed for observation in RS in the paramagnetic phase.

At the same time the energy of exchange magnons falls in the region of 50–300 cm^{-1} and Raman tensors for scattering on $\tilde{E}$ (or B') magnons contain both diagonal and nondiagonal components. High scattering intensity can be provided by a few factors: i) strong DM interaction which is necessary for observation of exchange magnons in Raman experiments [18]; ii) contribution of

exchange mechanism of Raman light scattering [19]; iii) existence of a few magnons with the same energy (quasi-degeneration caused by the restricted number of exchange integrals for the description of 15 exchange magnons). Our preliminary measurements of Cu_2OSeO_3 far-infrared (FIR) reflectance at 10 K [20] also demonstrate similar features in the same frequency region of spectra. Due to the above mentioned reasons the line at 420 cm^{-1} unambiguously has magnetic origin. For energy reason it can be attributed to two-magnon (TM) scattering in spite of its temperature behavior differs from *standard* TM temperature behavior in antiferro-magnets [21]. Because of the short-range-correlations, the TM RS in antiferromagnets persists at temperatures far above T_N contrary to our observations.

Intriguing is the appearance of two new lines at ~86 and 203 cm^{-1} in the Raman spectra (see Fig. 6,c and d) for temperatures below $T^* = 20$ K. Namely at this temperature the magnetic contribution to the dielectric constants change its sign [2]. We mentioned above that this change can be connected with a competing contribution from magnetic part of the CuI–CuII and CuII–CuII pair polarizability. The main exchange mechanism of magnon RS tensors also includes similar competing contributions from both pairs of ions which can be different for different type of exchange magnons. I.e., if we accept this hypothesis, then the observation of new magnon lines has an accidental
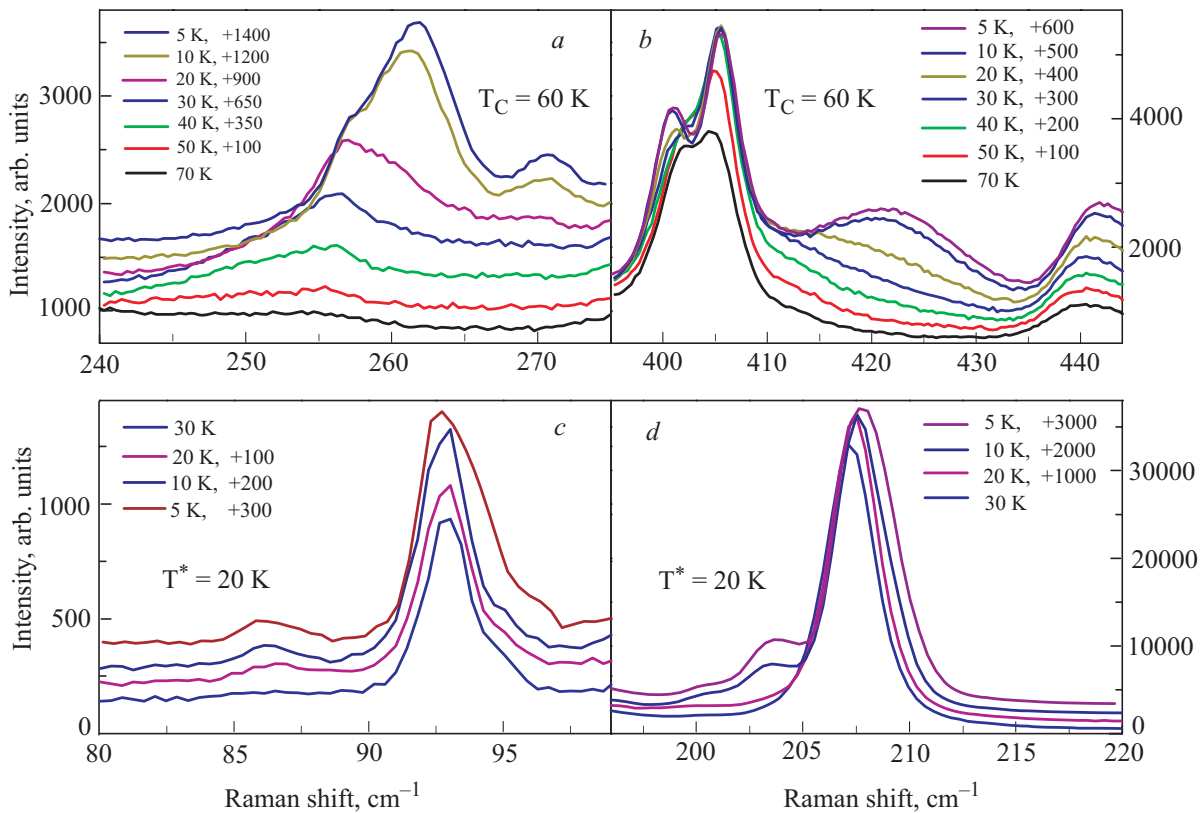

Fig. 6. Temperature evolution of the Raman spectra of Cu_2OSeO_3 in some selected frequency regions.

character connected with the special structure of Raman tensors.

However, one can suppose another mechanism for the appearance of those lines. The magnetic structure of Cu_2OSeO_3 shows some metamagnetic phase transition at very low fields [2]. In other words, there are two different ferrimagnetic structures which are very close in energy. New lines can be resolved in RS as a result of a spin-reorientation phase transition between these two ferrimagnetic phases under a decrease of temperature. In general, exchange modes are not sensitive to the orientation of magnetic structure in space, neither in energy, nor in their oscillation magnitude. Therefore, a part of them (at 261, 270 cm^{-1}) remains continuously seen in RS spectra.

Our phonon Raman spectra do not demonstrate any feature which could be interpreted as a manifestation of lattice strains induced by magnetic order. Indeed, in general ferrimagnetic order with net magnetic moment along (111) direction (unitary subgroup $R3$) should split the triply degenerate T modes and do not split the doubly degenerate E modes. Note, that for the case of our backscattering geometry this splitting of the polar T modes should lead just to a change of its already existing longitudinal-transversal splitting. While ferrimagnetic order with net magnetic moment along (100) direction (unitary subgroup $P2_1$) should completely split both T and E types of modes. However, we did not observe clear evidence of some additional splitting of the polar T modes, which we can surely identify in Raman spectra from our preliminary FIR measurements [20]. The absence of splitting means the absence of lattice distortions which, in its turn, do not appear if spontaneous electric polarization does not exist. Thus, we conclude on the ferrimagnetic order in Cu_2OSeO_3 occurring (at least at 10 K) with net magnetization along (100) direction, i.e., without the appearance of electric polarization, in accordance with (4). One can suppose that similarly to static measurements [2], strong magnetoelectric coupling in Cu_2OSeO_3 should directly prove itself in Raman spectra under the action of a magnetic field.

Some phonon frequencies show unusual temperature dependence below T_C. Typically phonons should demonstrate some hardening caused by a trivial renormalization due to spin phonon coupling in the form $\Delta\omega \propto \lambda\langle S_\alpha S_\beta\rangle$ [22]. In Fig. 5,*a* we present phonon frequencies which demonstrate both hardening and softening. A possible explanation of the strange softening could be related with phonons involving mainly vibrations of ions which realize magnetic bonds with angles closed to a critical ones (i.e., angles at which exchange integrals change sign). For instance, vibrations of O1 ions, which modulate the bond angle $\angle\,Cu1–O1–Cu1x = 104.72°$, can be candidates for this effect. Such a behavior one can

interpret as an internal instability of the magnetic subsystems which in its turn can be a possible reason for a spin reorientation phase transition. To make more definite statements we need lattice dynamic calculations which are now in progress.

Conclusions

Our Raman studies of the Cu_2OSeO_3, compound which possesses linear magnetoelectric effect, reveal the absence of structural lattice distortions at temperatures below T_C. This observation support the results of the low-temperature high-resolution x-ray and neutron powder diffraction measurements [2] which give no evidence for a structural change at T_C. Using a symmetry analysis we found a rather prosaic reason for this behavior, namely – if the net ferrimagnetic moment is directed along the cubic axes (for instance, along (100) or similar) than no spontaneous electric polarization appears. As discussed in the paper of J.-W. Bos *et al.* [2] such a model for the ferrimagnetic ground state is also in agreement with neutron diffraction data. At the same time the magnetocapacitive response observed in powder samples [2] can be easily achieved in a magnetic field under rotation of the net magnetic moment from (100) axis to the field direction. Thus the more general question for the relation of lattice distortions and electric polarization in multiferroics (i.e., the existence of a pure electronic mechanism of the magnetoelectricity) remains open.

An unusual demonstration of a dynamic magnetoelectric effect is observed as a strong enhancement of the phonon Raman scattering intensity below T_C. In other words, the dynamic ME effect leads to a general increase of the electric polarizability of the compound.

We show that the structural patterns of the Cu–O–Cu magnetic bonds allow strong Dzyaloshinskii–Moriya interactions and the net ferrimagnetic moment should be accompanied by the presence of antiferromagnetic vectors. We suppose that strong canting of the magnetic structure is the main reason of the small saturation moment per Cu ion seen in Cu_2OSeO_3 [2]. Observation of exchange magnon modes with scattering intensities compatible with phonon ones is an unambiguous evidence of strong DM interactions in Cu_2OSeO_3.

Appendix

Table A. The transformation properties of the Cu_2OSeO_3 magnetic degrees of freedom under symmetry operations of the paramagnetic phase $P2_13$ space group. The first column displays irreducible representations. Below we use notation $\varepsilon = \exp(i2\pi/3)$

IR	Magnetic basis functions	
	CuI	CuII
A	$L_{3x} + L_{1z} + L_{2y};$	$\Psi_{A1} = L_{3x}^{(z)} + L_{1z}^{(y)} + L_{2y}^{(x)};$ $\Psi_{A2} = L_{2y}^{(z)} + L_{3x}^{(y)} + L_{1z}^{(x)};$ $\Psi_{A3} = L_{1z}^{(z)} + L_{2y}^{(y)} + L_{3x}^{(x)}$
E_1	$\Psi_{E1} = L_{3x} + \varepsilon L_{1z} + \varepsilon^2 L_{2y}$	$\Psi_{E1(1)} = L_{3x}^{(z)} + \varepsilon L_{1z}^{(y)} + \varepsilon^2 L_{2y}^{(x)};$ $\Psi_{E1(2)} = L_{2y}^{(z)} + \varepsilon L_{3x}^{(y)} + \varepsilon^2 L_{1z}^{(x)};$ $\Psi_{E1(3)} = L_{1z}^{(z)} + \varepsilon L_{2y}^{(y)} + \varepsilon^2 L_{3x}^{(x)}$
E_2	$\Psi_{E2} = L_{3x} + \varepsilon^2 L_{1z} + \varepsilon L_{2y}$	$\Psi_{E2(1)} = L_{3x}^{(z)} + \varepsilon^2 L_{1z}^{(y)} + \varepsilon L_{2y}^{(x)};$ $\Psi_{E2(2)} = L_{2y}^{(z)} + \varepsilon^2 L_{3x}^{(y)} + \varepsilon L_{1z}^{(x)};$ $\Psi_{E2(3)} = L_{1z}^{(z)} + \varepsilon^2 L_{2y}^{(y)} + \varepsilon L_{3x}^{(x)}$
T	$\begin{Bmatrix} F_x \\ F_y \\ F_z \end{Bmatrix}; \begin{Bmatrix} L_{1y} \\ L_{3z} \\ L_{2x} \end{Bmatrix}; \begin{Bmatrix} L_{2z} \\ L_{1x} \\ L_{3y} \end{Bmatrix}$	$T_1 \Rightarrow \begin{Bmatrix} F_x^{(z)} \\ F_y^{(x)} \\ F_z^{(y)} \end{Bmatrix} \quad T_2 \Rightarrow \begin{Bmatrix} L_{2z}^{(y)} \\ L_{1x}^{(z)} \\ L_{3y}^{(x)} \end{Bmatrix}; \quad T_3 \Rightarrow \begin{Bmatrix} L_{1y}^{(x)} \\ L_{3z}^{(y)} \\ L_{2x}^{(z)} \end{Bmatrix};$ $T_4 \Rightarrow \begin{Bmatrix} L_{1y}^{(z)} \\ L_{3z}^{(x)} \\ L_{2x}^{(y)} \end{Bmatrix}; \quad T_5 \Rightarrow \begin{Bmatrix} F_x^{(y)} \\ F_y^{(z)} \\ F_z^{(x)} \end{Bmatrix}; \quad T_6 \Rightarrow \begin{Bmatrix} L_{2z}^{(x)} \\ L_{1x}^{(y)} \\ L_{3y}^{(z)} \end{Bmatrix};$ $T_7 \Rightarrow \begin{Bmatrix} L_{2z}^{(z)} \\ L_{1x}^{(x)} \\ L_{3y}^{(y)} \end{Bmatrix}; \quad T_8 \Rightarrow \begin{Bmatrix} L_{1y}^{(y)} \\ L_{3z}^{(z)} \\ L_{2x}^{(x)} \end{Bmatrix}; \quad T_9 \Rightarrow \begin{Bmatrix} F_x^{(x)} \\ F_y^{(y)} \\ F_z^{(z)} \end{Bmatrix}.$

1. K. Kohn, *J. Phys. Soc. Jpn.* **42**, 2065 (1977).

2. Jan-Willem G. Bos, Claire V. Colin, and Thomas T.M. Palstra, *Phys. Rev.* **B78**, 094416 (2008).

3. H. Effenberger and Pertlik, *Monatshefte für Chemie* **117**, 887 (1986).

4. G. Meunier, M. Bertaud, and J. Galy, *J. Appl. Cryst.* **9**, 364 (1976). In this Ref. the crystal structure of Cu_2OSeO_3 had been determined as cubic with space group $P2_13$ or $P4_232$.

5. S. Picozzi and C. Ederer, *J. Phys.: Condens. Matter* **21,** 303201 (2009).

6. L.C. Chapon, G.R. Blake, M.J. Gutmann, S. Park, N. Hur, P.G. Radaelli, and S.W. Cheong, *Phys. Rev. Lett.* **93**, 177402 (2004).

7. C. dela Cruz, F. Yen, B. Lorenz, Y.Q. Wang, Y.Y. Sun, M.M. Gospodinov, and C.W. Chu, *Phys. Rev.* **B71**, 060407(R) (2005).

8. C.R. dela Cruz, F. Yen, B. Lorenz, M.M. Gospodinov, C.W. Chu, W. Ratcliff, J.W. Lynn, S. Park, and S.-W. Cheong, *Phys. Rev.* **B73**, 100406(R) (2006).

9. S. Lee, A. Pirogov, M. Kang, K.-H. Jang, M. Yonemura, T. Kamiyama, S.W. Cheong, F. Gozzo, N. Shin, H. Kimura, Y. Noda, and J.-G. Park, *Nature* (*London*) **451**, 805 (2008).

10. E. Montanari, G. Calestani, L. Righi, E. Gilioli, F. Bolzoni, K.S. Knight, and P.G. Radaelli, *Phys. Rev.* **B75**, 220101(R) (2007).

11. G. Güntherodt and R. Zeyher, Spin-dependent Raman scattering in magnetic semiconductors, in *Light Scattering in*

Solids IV: Electronic Scattering, Spin Effects, SERS, and Morphic Effects, *Topics Appl. Phys.* **54,** Springer, Berlin, Heidelberg (1984).

12. Y. Mizuno, T. Tohyama, S. Maekawa, T. Osafune, N. Motoyama, H. Eisaki, and S. Uchida, *Phys. Rev.* **B57**, 5326 (1998).

13. C. de Graaf, I. de P.R. Moreira, F. Illas, O. Iglesias, and A. Labarta, *Phys. Rev.* **B66**, 014448 (2002).

14. V. Gnezdilov, P. Lemmens, A.A. Zvyagin, V.O. Cheranovskii, K. Lamonova, Yu.G. Pashkevich, R.K. Kremer, and H. Berger, *Phys. Rev.* **B78**, 184407 (2008).

15. G.A. Smolenskii and I.E. Chupis, *Usp. Fiz. Nauk* **137,** 415 (1982) [*Sov. Phys. Usp.* **25,** 475 (1982)].

16. I.M. Vitebskii, N.M. Lavrinenko, and V.L. Sobolev, *J. Magn. Magn. Mater* **97**, 263 (1991).

17. Yu.G. Pashkevich and S.A. Fedorov, *Ukr. Phys. J.* **38**, 279 (1993) (in Russian).

18. Yu.G. Pashkevich, V.L. Sobolev, and S.A. Fedorov, *J. Phys. C: Solid State Phys.* **21**, 1265 (1988).

19. Yu.G. Pashkevich, V.L. Sobolev, S.A. Fedorov, and A.V. Eremenko, *Phys. Rev.* **B51**, 15898 (1995).

20. V. Tsapenko *et al.* (unpublished).

21. M.G. Cottam and D.J. Lockwood, *Light Scattering in Magnetic Solids,* Wiley, New York (1986).

22. W. Baltensperger and J.S. Helman, *Helv. Phys. Acta* **41**, 668 (1968).